Atmospheric Environment Vol. 24A, No. 7, pp. 1801–1811, 1990.
Printed in Great Britain.

0004-6981/90 $3.00 + 0.00
Pergamon Press plc

ON THE EFFECT OF DAYTIME SURFACE EVAPORATION ON POLLUTION DISPERSION

M. SEGAL,* X. JIA,† Z. YE† and R. A. PIELKE
Department of Atmospheric Science, Colorado State University, Fort Collins, CO 80523, U.S.A.

(*First received* 1 *February* 1989 *and in final form* 29 *December* 1989)

Abstract—The general effects of surface moisture availability on regional and local pollution dispersion during the day are examined through conceptual modeling and analytic analysis, when surface moisture availability is assumed to be homogeneous over regional scales. The results suggest that in low mid-latitudes and sub-tropical regions the change in Pasquill stability classes around noon, between extremely wet and very dry surfaces, is typically one stability class shift. In the morning and the afternoon, however, the corresponding change is more pronounced. Similar trends were suggested when the evaluations were made in terms of w^*/U (where w^* is the convective scaling velocity and U the mean wind speed within the daytime convective boundary layer). Also, numerical model simulations and analytical evaluations were carried out providing an estimation of the mixing layer depth as dependent on the surface moisture availability. The mixing layer depth over extremely dry surfaces was found to be $\sim$ 1.5–2 higher compared to that computed over very wet surfaces. Observational aspects are discussed, suggesting complementary insight into the interpretation of the modeling and the analysis results.

Key word index: Pollution dispersion, surface evaporation, convective boundary layer.

1. INTRODUCTION

Dispersion of pollutants from surface emissions along relatively short distances is commonly evaluated utilizing the well-known 'σ' curves (e.g. Pasquill–Gifford) which are related to the Pasquill stability classes. The Pasquill stability classes are specified during the day hours based on surface wind speed, three levels of the amount of the solar radiation in addition to the amount of cloud cover. Golder (1972) provided a more rigorous way to identify the Pasquill stability classes, where they are related to the magnitude of z_0 (the surface roughness height) and L^{-1} (L is the Monin–Oboukov length). The magnitude of L is affected by the sensible heat flux (H_s) and the shearing stress at the surface layer. The magnitude of H_s depends on several environmental parameters including solar radiation, surface albedo, surface wind speed, surface moisture, etc. Therefore, expressing the Pasquill stability classes by means of Golder's relations, enables their adequate utilization for specific environmental conditions. More adequate, however, is scaling the dispersion in terms of characteristic boundary layer parameters. Weil and Brower (1984) and Briggs (1988), for example, suggested utilizing the ratio w^*/U (where w^* is the convective scaling velocity and U is the mean wind speed within the daytime convective boundary layer), as a physical index for the dispersion in the daytime boundary layer.

Evapotranspiration is a major cause of the modification in H_s during the daytime. Grossly for bare soil, H_s can be evaluated through the relation

$$H_s \cong R_S - H_L - \beta \tag{1a}$$

$$\beta = R_{LN} + G \tag{1b}$$

where R_S is the absorbed solar radiation at the surface, H_L is the evapotranspiration thermal flux, R_{LN} is the net long wave radiation and G is the soil thermal flux at the surface. Denoting by R_N the net radiation at the surface, then over bare soil $G \leqslant 0.3\ R_N$ (e.g. Brutsaert, 1982), while, for a densely vegetated surface approximately $G \cong 0$ in Equation (1). For a given geographical location, time of year, and hour, grossly $R_S - \beta$ can be considered as a constant (assuming clear sky conditions). Therefore, it is anticipated that modification of surface evaporation caused, for example, by moistening of soil by precipitation (or equivalently due to canopy transpiration) would affect the value of H_s. As a result the following is suggested.

(i) The value of L^{-1} and the related surface dispersion characteristics would also be modified. Although daytime evaporation thermal effects on the atmosphere are likely to be significant in many surface dispersion situations, apparently no corresponding attention has been given to evaluate quantitatively its general impact. An exception is the study by Myrup and Ranzieri (1976) which suggested qualitative estimates of the impact of evaporation on the Pasquill stability classes.

Since the Pasquill stability classes can be established by readily available meteorological data, they are commonly adopted in many applied studies. Evaluation of the impact of surface wetness conditions

* Present address: Department of Physics and Astronomy, University of Kansas, KS 66045, U.S.A.
† Permanent address: Institute of Atmospheric Physics, Academia Sinica, Beijing, China.

on the Pasquill stability classes will enable a corresponding adjustment in such applied studies.

(ii) The Pasquill classes correlation with L^{-1} should be viewed as applicable for relatively short distances from the source, and for evaluating vertical dispersion from near ground sources. For all other daytime dispersion conditions involved with relatively long distances, lateral dispersion, or elevated sources, a physical index characterizing the diffusion rate is required. In the present study we also adopted, following Weil and Brower (1984) and Briggs (1988), the ratio w^*/U as such index while evaluating the impact of surface wetness on dispersion. It should be pointed out, however, that the usage of this index in applied studies is likely to be limited since the meteorological data needed for computing its climatology are, generally, unavailable.

(iii) The ABL is well-known to be in many situations a trapping layer for elevated emissions and to a certain degree also for surface layer emissions. Some aspects of the impact of soil wetness on the depth of the ABL, h, were investigated by numerical modeling means by Zhang and Anthes (1982), and Pan and Mahrt (1987). Zhang and Anthes (1982) found that variations within the lower range in surface moisture availability over uniform areas lead to a more pronounced change in the depth of the ABL as compared to that involved with a typical range of changes in the albedo, surface roughness and soil conductivity. In the present study, several illustrative model simulations and general analytic evaluations were carried out in order to generate a nomogram which illustrates a general scaling of the impact of soil moisture on h.

It is the purpose of the present study to provide a quantification of dispersion characteristics as related to (i)–(iii) above. The model outlined in section 2 is adopted for the evaluations, where a summer day and a winter day are considered. Thus, high and low level solar radiation conditions are involved with the presented simulations. The study focuses on the daylight hours in which the evapotranspiration rates are generally considerably higher as compared to the nocturnal period and therefore the possible errors in their estimation should not significantly influence the conclusions. The evaluations are related to horizontal homogeneous areas in which the diurnal and the seasonal surface soil moisture availability variations are assumed to be linked to the precipitation or irrigation characteristics.

2. THE MODEL

2.1. *The atmospheric model*

The numerical mesoscale model, whose formulation is given in Mahrer and Pielke (1977) and McNider and Pielke (1981), is adopted for the simulations in section 3. Since a detailed description of the atmospheric model appears in these papers only a brief description of this model is given in the present paper.

Over flat terrain, assuming horizontal homogeneity for $\vec{V}$, θ, R and q, the prediction equations for wind velocity, $\vec{V}$, the potential temperature, θ, and moisture, q, are:

$$\frac{\partial \vec{V}}{\partial t} = f\vec{k} \times (\vec{V}_g - \vec{V}) + \frac{\partial}{\partial z}\left[K_M \frac{\partial \vec{V}}{\partial z}\right] \tag{2}$$

$$\frac{\partial \theta}{\partial t} = \frac{\partial}{\partial z}\left[K_H \frac{\partial \theta}{\partial z}\right] + R \tag{3}$$

$$\frac{\partial q}{\partial t} = \frac{\partial}{\partial z}\left[K_Q \frac{\partial q}{\partial z}\right] \tag{4}$$

where $\vec{V}_g$ is the geostrophic wind, f is the Coriolis parameter, and R is the radiation heating/cooling term. K_M, K_H and K_Q are the vertical eddy diffusion coefficients for momentum, heat and specific humidity, respectively.

Parameterizations within the atmospheric model include calculations of the surface fluxes of momentum, heat and moisture according to Businger *et al.* (1971). The eddy diffusion coefficients in the ABL above the surface layer are of the O'Brien (1970) functional form. A prognostic equation is solved to predict the value of h. The changes of air temperature, due to shortwave and longwave radiative flux divergence, are parameterized following the methods of Atwater and Brown (1974), and Sasamori (1972). Heating of the atmosphere by shortwave radiation is confined to absorption by water vapor, while carbon dioxide and water vapor are both considered in the longwave radiation heating–cooling algorithm.

The model was validated in a variety of studies which indicated reasonable prediction skills (e.g. Pielke and Mahrer, 1978; Segal and Mahrer, 1979; Segal and Pielke, 1981, among others).

2.2. *The soil model*

In this paper only brief details relating to the soil layer will be given. The soil modeling consists of solving the equation for thermal conduction

$$\rho_s C_s \frac{\partial T}{\partial t} = \lambda \frac{\partial^2 T}{\partial z^2} \tag{5}$$

with $\lambda = \rho_s C_s k_s$ where T is the soil temperature, ρ_s the soil density, C_s the soil heat capacity, λ the soil heat conductivity and k_s the soil heat diffusivity coefficient. In the present study a sand type of soil is assumed. The soil heat fluxes for most other types of soils are suggested to be not too different from those computed for sand.

The surface soil moisture availability, m, is assumed to be homogeneous with depth and its contribution to the surface value of the specific humidity (of the air), $q(z_0)$ is given according to

$$q(z_0) = q(z_1)(1-m) + mq_s(z_0) \tag{6}$$

where $q_s(z_0)$ is the saturated specific humidity at the temperature of the surface, T_s; $q(z_1)$ is the specific

humidity at the first level of the model; m is defined as

$$m = \frac{E}{E_p}, \tag{7}$$

where E and E_p are the actual and the potential evaporation rates at the surface, respectively. The relation in Equation (6) or its variants have been adopted in various studies (e.g. Nappo, 1975; Carlson and Boland, 1978, among others). In the evaluations presented in this study a relation between m and the Bowen ratio was established as discussed in section 4.1. This enables the interpretation of the results also as dependent on the Bowen ratio. When the soil is absolutely dry its contribution to the value of the $q(z_0)$ is zero. Since $q(z_1) > 0$, the initial moisture gradient towards the surface eventually should result in $q(z_0) = q(z_1)$ (obviously during the daytime no dew is formed, while the soil is a negligible sink to that moisture flux). When $q(z_0) = q(z_1)$, no surface latent heat flux atmosphere exists as anticipated in the case of a dry soil surface.

The temperature at the soil–air interface is calculated as a function of time using a thermal balance equation which includes solar radiation, incoming longwave radiation, latent, sensible and soil heat fluxes and the outgoing surface longwave radiation.

It is worth noting that McCumber and Pielke (1981) introduced into the present model a detailed formulation for soil physics. However, since in the current study we desire only a general estimate of the sensitivity of the simulated dispersion characteristics to soil moisture a simplified routine for the soil formulation is appropriate.

Parameterization of the effects of soil moisture availability on the albedo, soil heat capacity, and diffusivity are included in a similar manner to that reported in Ookouchi *et al.* (1987) (although generally the inclusion of these effects in detail was found to result in only marginal modifications on most of the results presented in the next section). Since for this parameterization the soil volumetric moisture is needed, the following approximations were made: (i) $m = 0$ indicates absolutely dry soil (e.g. in arid regions, or during a drought), corresponding to a volumetric soil moisture of 0%; (ii) $m = 1$ reflects saturated soil (e.g. following a heavy rainfall event) which corresponds in the current study to a 40% volumetric soil moisture in a sandy type of soil; (iii) intermediate volumetric soil wetness values were approximated linearly between these two extremes based on the value of m (i.e. $\eta = m \cdot \eta_s$, where η is the actual soil volumetric wetness and η_s is the corresponding saturated volumetric soil wetness). During the simulation period in the present study, m is assumed to be constant. To evaluate the relatively secondary effect of soil moisture on albedo (α), we adopted the following relation (Idso *et al.*, 1975);

$$\alpha = 0.31 - 0.17 \cdot \frac{\eta}{\eta_s}. \tag{8}$$

The dependence of soil heat capacity and diffusivity on soil moisture and temperature are calculated according to De Vries (1963).

3. EVALUATIONS

3.1. *The impact of surface wetness on the Pasquill classification*

A large area with homogeneous surface moisture availability and terrain features is assumed. In this case, an application of the one-dimensional model version is appropriate for the evaluation of the development of the daytime surface layer and the ABL for that region. A bare soil surface is assumed in these evaluations. The implication of the simulated features for different surface conditions are discussed in section 4.3.

The daytime stability classification according to Pasquill is related to the intensity of the incoming solar radiation which influences the surface layer turbulence intensity. Clouds and increased surface wetness result in a reduction in the surface sensible heat fluxes and consequently in the turbulence intensity. The midday largest possible shift in the Pasquill stability classification because of cloudiness variations is about one stability class. A change of this order is also likely with an extreme change of the surface wetness. This change is suggested by Myrup and Ranzieri (1976) while considering low surface evaporation vs very high surface evaporation (see Fig. 1).

However, when solar radiation incoming at the surface is suppressed because of a heavy overcast or when the sun angle is low, based on Turner's (1964) classification, a more noticeable change in the stability classes is likely to occur. In the early morning and late afternoon under extensive cloudiness the surface net radiation may become negative and an otherwise unstable Pasquill class may turn to a stable one. The impact on the Pasquill classes of a change from dry soil into a saturated soil would be expected to be similar. The influence on pollutant dispersion in such situations is suggested, therefore, to be noticeable.

Figures 2–5 present simulation results designed to evaluate the impact of various surface wetness and its temporal variations on surface layer stability and Pasquill classes. The evaluations are based on a set of simulations using Equations (2)–(5) in section 2 with a combination of roughness parameters: $z_0 = (0.01, 0.05$ m) and soil wetness availability $m = (0.01, 0.05, 0.10, 0.50$ and $1.00)$. A summer day case (15 August; latitude 32° N) with a geostrophic wind of $V_g = (3, 5$ and 7 m s^{-1}) within the ABL (Figs 2a–b, 3a–b and 4a–b), as well as an illustrative winter day case (1 January; latitude 32° N) with a geostrophic $V_g = 3$ m s^{-1} within the ABL (Fig. 5a) are considered. The initial profiles (0600 LST) of the potential temperature and the specific humidity are given in Table 1. The soil moisture availability, m, reflects the range between an extremely

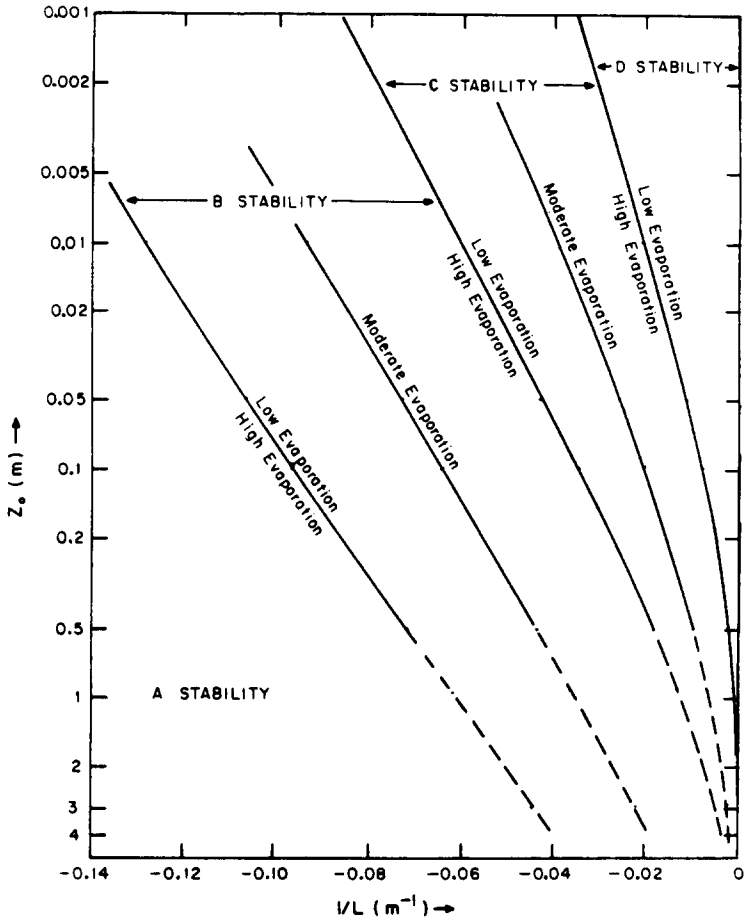

Fig. 1. Pasquill stability classes as dependent on L^{-1}, z_0 and the surface evaporation intensity for unstable surface layer conditions (reproduced from Myrup and Ranzieri, 1976).

Table 1. Initial profiles of the potential temperature, θ, and the specific humidity, q, used in the numerical model simulations

season	variable	Level (m)													
		10	32.5	75	200	400	600	800	1050	1350	1750	2500	4000	6000	7000
summer	$\theta(K)$	293 K at the surface; $\frac{\partial\theta}{\partial z} = 3.5$ K km^{-1}													
	q(gr kg^{-1})	12.5	12.5	12.5	12.5	12.5	12.5	8.5	8.0	5.5	4.2	1.2	1.2	1.2	1.2
winter	$\theta(K)$	283 K at the surface; $\frac{\partial\theta}{\partial z} = 3.5$ K km^{-1}													
	q(gr kg^{-1})	6.3	6.3	6.3	6.3	6.3	6.3	4.3	4.0	2.8	2.1	0.6	0.6	0.6	0.6

dry surface to a nearly saturated surface. Based on the nomogram provided in Myrup and Ranzieri (1976) (which is an extension of the Golder (1972) nomogram), for given values of z_0 and model computed values of L^{-1} the related Pasquill stability classes were determined.

The results suggest the following: (i) the maximum change in the Pasquill stability class as a result of extreme changes in surface moisture is a shift by one stability class during most of the daytime hours [this is in support of the Myrup and Ranzieri (1976) suggestion]; (ii) as z_0 and the surface wind speed reduce, the impact of surface moisture on the change in the Pasquill stability classes also is reduced; (iii) the change from a stable surface layer into an unstable layer (i.e. change to $L^{-1} < 0$) during the morning hours is lagged in time (up to 1–2 h) as soil moisture availability increases. Around sunset the change from unstable surface layer into a stable surface layer (e.g. $L^{-1} > 0$) occurs earlier by 1 to 2 h when soil wetness is higher. In these periods the impact of an extreme change in the soil moisture availability is likely to be expressed by a shift in more than one Pasquill stability class; and (iv) Around noon hour, somewhat more noticeable stabilization is computed in the winter as compared with the summer case.

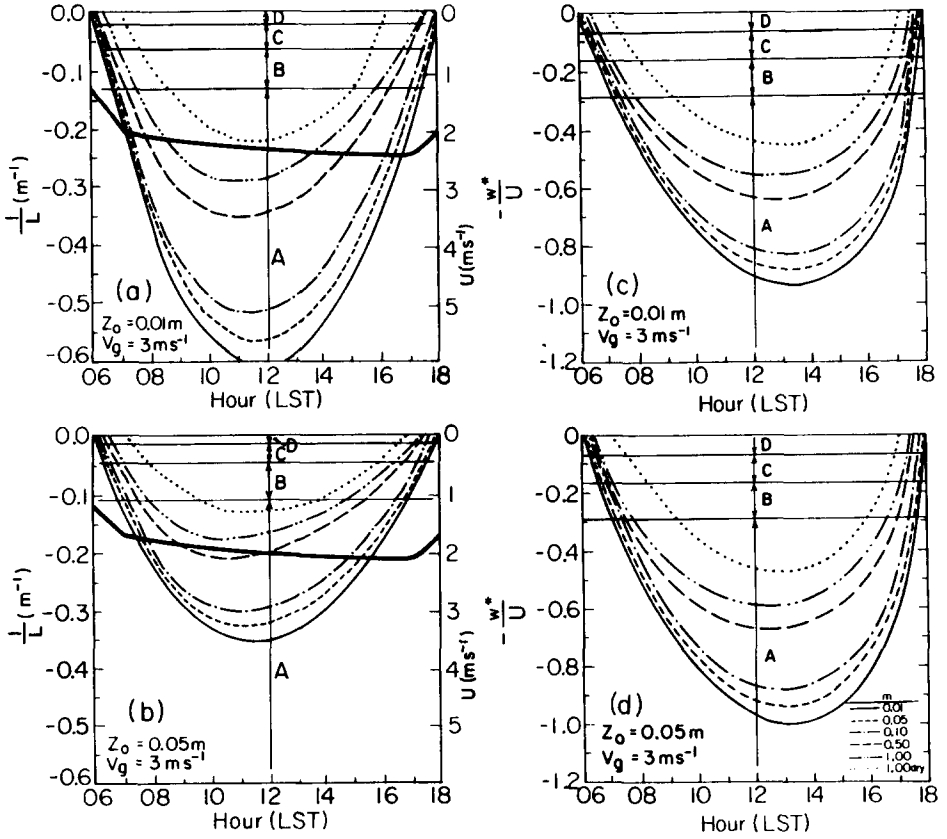

Fig. 2(a–b). The numerical model predicted temporal variation of L^{-1} during the summer daytime for the indicated combination of surface moisture availability, m (the curve: $m = 1.00$ dry, indicates a simulation in which the atmospheric initial specific humidity was reduced to 20% of its value specified in Table 1), surface roughness height, z_0, of 0.01 and 0.05 m and $V_g = 3$ m s^{-1}. The corresponding ranges of Pasquill stability classes (as suggested by Fig. 1) are indicated. Dark lines indicate the daytime variation of the wind speed at 5 m for $m = 0.05$. (c–d) are the same as (a–b) except for the temporal variation of $-w^*/U$, and using the stability classification adopted from Weil and Brower (1984).

3.2. *The impact of surface wetness on* w^*/U

Similar to the evaluation of the impact of the surface wetness on the Pasquill stability classes, corresponding evaluations were carried out for the impact of wetness on w^*/U. The value of the convective scaling velocity w^*, is given by:

$$w_* = \left(\frac{g H_s h}{\rho C_p \theta_0}\right)^{1/3} \tag{9}$$

where g is the gravity acceleration, H_s is the surface sensible heat flux, ρ is the air density, C_p is the specific heat of the air at constant pressure, and θ_0 is the background air potential temperature. U is the mean wind speed within the daytime convective ABL. Obviously, the magnitude of H_s and h reduce with an increase in the surface wetness. Thus, the value of w^* also decreases with an increase in the surface wetness (see discussion in section 4.2). On the other hand, a quite mild effect due to variations in the surface wetness is involved with U, where, typically, the value of U is somewhat lower than the corresponding value of V_g.

Figures 2c–d, 3c–d, 4c–d and 5b present the dependence of $-w^*/U$ on m, z_0 and V_g as computed for the same numerical model simulations discussed previously. In order to provide a reference for evaluating the impact of variations in the surface wetness on $-w^*/U$, Brigg's dispersion curves classification was adopted, where the related range of dispersion in terms of $-w^*/U$ was adopted from Table 1 in Weil and Brower (1984) (A—extremely unstable layer; D—neutral layer). As is evident from the figures, the following is suggested: (i) at noon and for low V_g values, moistening of the surface results in a reduction in the value of $-w^*/U$, which is expressed, however, merely by a moderation of the Brigg's curve class A. For the high value of wind speed V_g ($= 7$ m s^{-1}), increased surface wetness resulted in a less unstable Brigg's curve class at noon; (ii) during the morning and in the late afternoon hours, the impact of a variation in the surface wetness on Brigg's curves classes is more noticeable as compared to the noon hour; and (iii) the value of $-w^*/U$ is almost unaffected by the change in z_0 (unlike L^{-1}). This feature is explained by the dependence of w^* on H_s (i.e. $w^* = w^*(H_s, h(H_s))$),

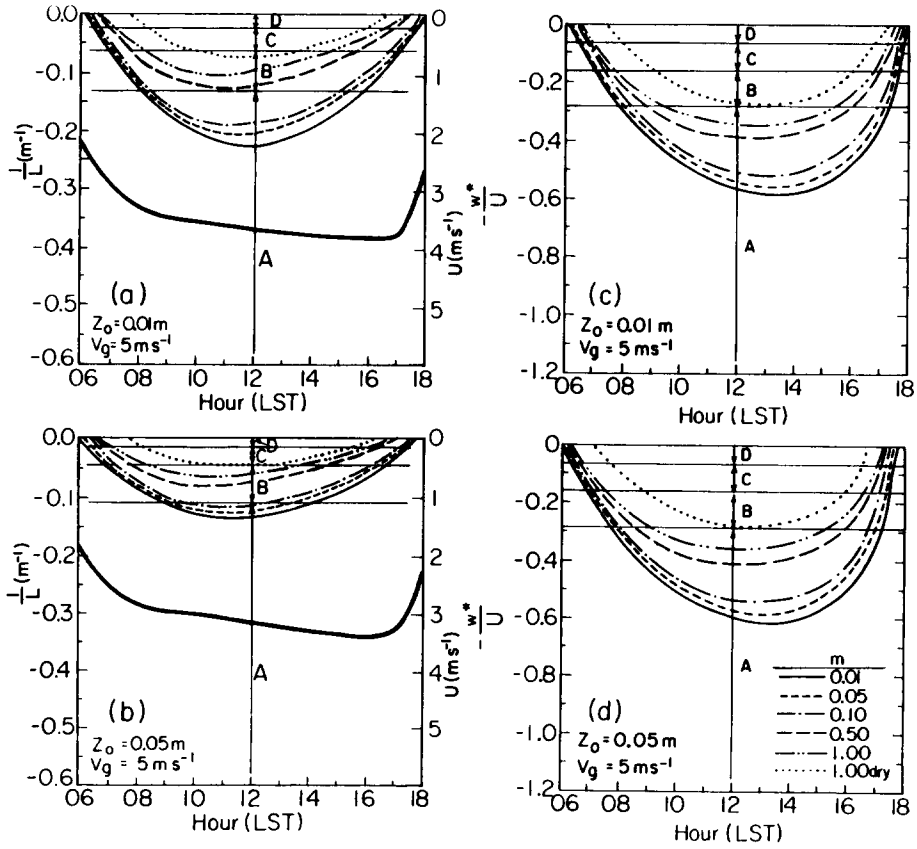

Fig. 3. The same as Fig. 2, except for $V_g = 5\ \mathrm{m\ s^{-1}}$.

where the variations of H_s with a change of z_0 are quite mild. Similarly, U is affected only slightly by the changes in z_0 as adopted in our simulation.

3.3. *Surface moisture effect on the development of the ABL*

3.3.1. *Numerical model results.* The value of h is a major parameter involved with a daytime dispersion assessment. It is important to consider its characteristics during daytime trapping conditions involved with an elevated plume, or as an input parameter for pollutants dispersion box models.

The daytime evaluation of the ABL as dependent on surface moisture availability, m, is presented through several illustrative numerical model simulations, which were carried out for summer and winter daytime hours (Fig. 6). Relatively accelerated growth of h is simulated until the early afternoon hours, which was followed by slow changes in the late afternoon hours (mostly for the highly wet surfaces). The value of h as dependent on m increased gradually as soil moisture availability was decreased in the simulations. By the end of the summer simulated day, h, is larger by ~ 1.9 for $m = 0.01$ as compared to that computed for $m = 1.0$, while for the winter case the corresponding ratio was ~ 1.6.

3.3.2. *Analytical results.* In order to provide general scaling for the impact of wet soil on the development of the daytime ABL the following evaluations are adopted. Using an encroachment assumption, the depth of the daytime ABL, h_t, at time, t, following the initiation of sensible heat fluxes into the atmosphere can be estimated as (e.g. Tennekes, 1973):

$$h_t \cong \left[\frac{2\int_0^t H_s\,dt}{\rho C_p \dfrac{\partial\theta_0}{\partial z}}\right]^{1/2} \tag{10}$$

where $\partial\theta_0/\partial z$ is the potential temperature gradient within the lower atmosphere at sunrise. Note, however, that observed potential temperature vertical gradients at sunrise decrease somewhat with height. Thus, $\partial\theta_0/\partial z$ reflects a scaled value for this gradient. For scaling purposes we can estimate H_s utilizing Equation (1).

In the present study it is assumed, as closely observed during clear sky conditions (e.g. Hillel, 1982; Stull, 1988), that:

$$\begin{bmatrix} R_s \\ \beta \\ H_L \end{bmatrix} = \begin{bmatrix} R_{s_0} \\ \beta_0 \\ H_{L_0} \end{bmatrix} \sin\left(\frac{\pi t}{T}\right) \tag{11}$$

where R_{s_0}, β_0 and H_{L_0} are the noon hour values of R_s,

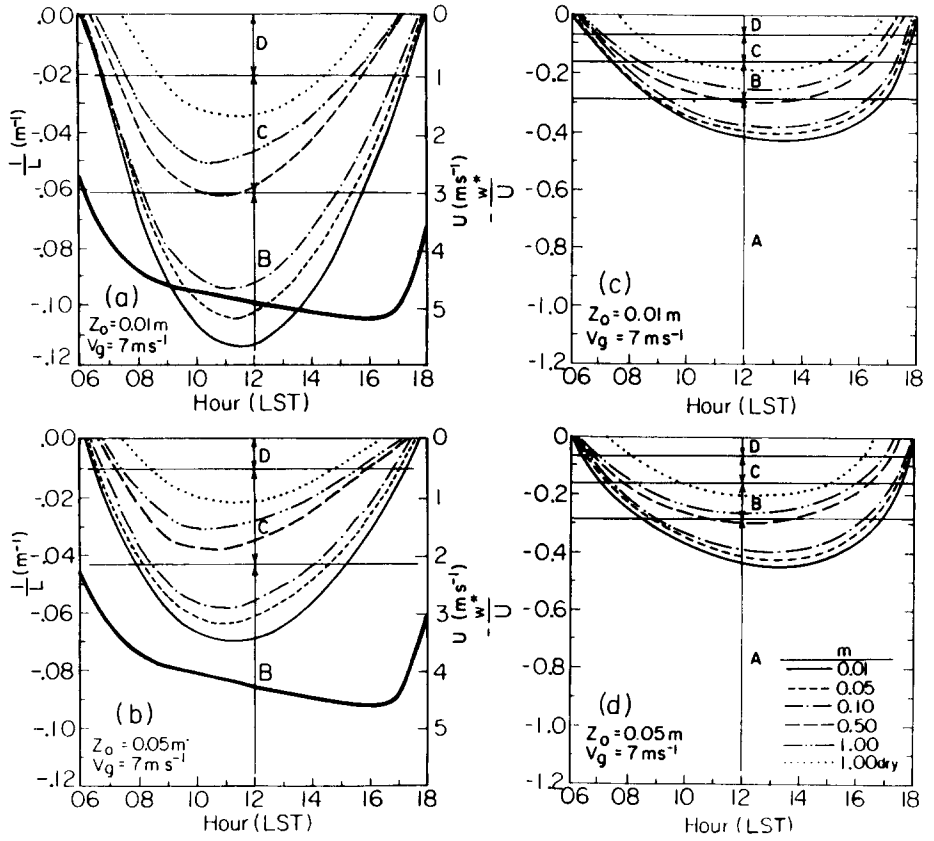

Fig. 4. The same as Fig. 2, except for $V_g = 7$ m s^{-1}.

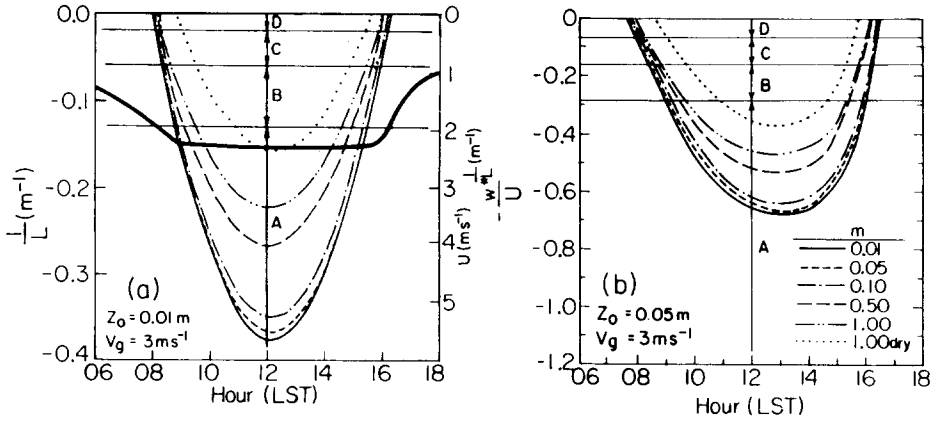

Fig. 5. The same as Fig. 2, except for winter daytime and only for $z_0 = 0.01$ m and $V_g = 3$ m s^{-1}.

β and H_L, respectively, and T is the duration of the sunny hours (here $t = T/2$ at noon). Substituting Equation (11) into Equation (10) and integrating results in:

$$h_t \cong \left[\frac{2\frac{T}{\pi}(R_{s_0} - H_{L_0} - \beta)\left(1 - \cos\left(\frac{\pi t}{T}\right)\right)}{\rho C_p \frac{\partial \theta_0}{\partial z}}\right]^{1/2}. \quad (12)$$

Assuming (as computed in the numerical simulations), a mid-latitude clear summer day with $R_{s_0} \cong 780$ W m^{-2} and a midwinter clear day with $R_{s_0} \cong 480$ W m^{-2}, and $\partial\theta_0/\partial z = 3.5$ K km^{-1} m, daily variations of h_t were computed for various values of H_{L_0}. The surface evaporation rate, H_L, expressed by F, is defined as:

$$F = H_L/(R_s - \beta) = H_{L_0}/(R_{s_0} - \beta_0) = \frac{1}{1+B} \quad (13)$$

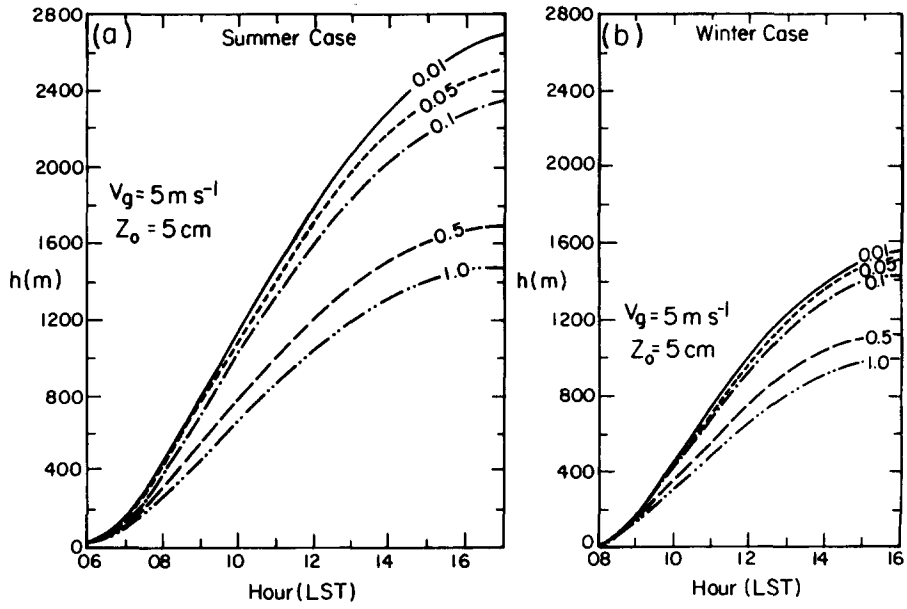

Fig. 6. The numerical model predicted ABL heights as a function of time for $V_g = 5\ m\ s^{-1}$; $z_o = 5$ cm and the indicated values of the soil moisture availability, m. (a) summer case (15 August sun conditions) and (b) winter case (1 January sun conditions).

where B is the Bowen ratio ($B = H_s/H_L = H_{s_0}/H_{L_0}$). Thus, for an absolutely dry surface (i.e. $H_L = 0$), $F = 0$; for a very wet surface $B \ll 1$ and $F \to 1$.

Equation (12) can be rewritten as:

$$h_t \cong \left[\frac{\frac{2}{\pi}\frac{T}{\pi}(1-F)(R_{s_0}-\beta_0)\left(1-\cos\left(\frac{\pi t}{T}\right)\right)}{\rho C_p \frac{\partial\theta_0}{\partial z}}\right]^{1/2}. \tag{14}$$

Based on a set of simulations for summer and winter conditions with the numerical model, which were reported in section 3.3.1, the values of β_0 (as given in Equation 1b) and that of F (as given by Equation (13), using simulated values of B) were computed. Based on these data it was found that β_0 can be approximated linearly as:

$$\beta_0 = \begin{cases} 330 - 130F & \text{W m}^{-2}\text{; summer case} \\ 230 - 90F & \text{W m}^{-2}\text{; winter case.} \end{cases} \tag{15}$$

The evaluation of the ABL depth, h_t, as dependent on m and the time of the day, using the analytical solutions given in Equation (14), for the summer and the winter days is presented in Fig. 7. Using Equation (13) and the relation between B and m as suggested by Fig. 8 enables comparisons of the analytical results (Fig. 7) with the numerical results for h, presented in Fig. 6. Considering the bulk approximations involved with the analytical scaling a general agreement between both evaluations of h_t is found. For example, for the summer case at 1700 LST for $m = 0.01$ (which corresponds to $F \cong 0.06$), in the numerical model $h_t \cong 2700$ m as compared to $h_t \cong 2400$ m based on the analytical computations. In the winter for this surface wetness the related values are 1400 m and 1470 m, respectively. Assuming $m = 1$ (which corresponds to $F \cong 0.8$) in the summer day at 1700 LST, the numerical model simulations suggest $h_t \cong 1400$ m as compared to $h_t \cong 1150$ m derived in the analytical evaluation. In the winter case the respective values at 1600 LST are $h_t = 970$ m and 740 m.

4. SOME GENERALIZATIONS

4.1. *Bowen ratio*

In order to enable use of the numerical model and the analytical results presented in this paper for evaluations of the impact of real world wet surfaces on dispersion, it is advantageous to establish a simplified measure expressing the degree of the surface wetness. Most attractive is to carry out such an estimation through the magnitude of the Bowen ratio, B, which has been documented in many observational studies, and which can be estimated based on simple measurements. Measurements needed for computation of B have to include the air potential temperature and specific humidity at two different heights within the surface layer. This approach for evaluating the Bowen ratio provides quite accurate results while applied during the daytime hours. Numerous studies report on observed values of B and their sensitivity to the surface temperature and moisture. Summaries of these study results can be found in Monteith (1976), Hillel (1982) and Stull (1988) among others. A useful nomogram evaluating the physical bound of B as dependent

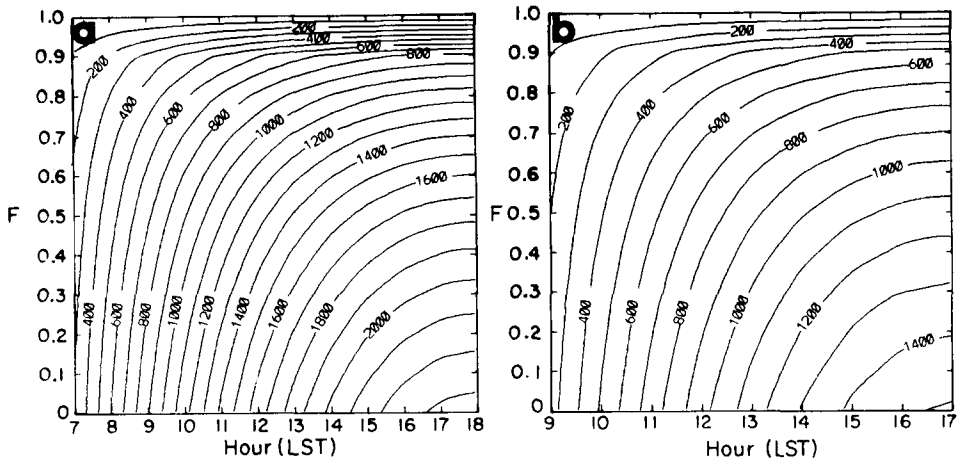

Fig. 7. The variation of the ABL height with time (based on Equation 14) as dependent on surface latent heat fluxes as expressed through F (see Equation 13) for: (a) a mid-latitude clear summer day with $R_{s_0} = 780$ W m^{-2}, and (b) a mid-latitude clear winter day with $R_{s_0} = 480$ W m^{-2}.

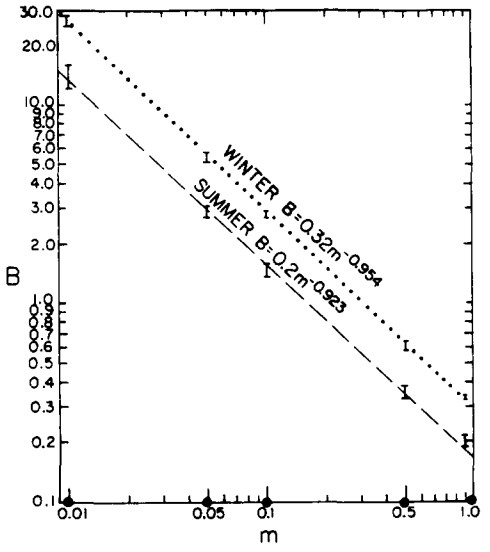

Fig. 8. The dependence of the Bowen ratio, B, on the surface moisture availability, m, based on the numerical model simulations present in section 3. The vertical lines scale the variation of B for the z_0 and V_g values given in Figs 2–5.

on the surface temperature and the surface wetness is given in Philip (1987). A relation between the surface moisture availability, m, and the computed Bowen ratio in the one-dimensional simulations presented in section 3.1, is established in Fig. 8. It was found from the results of these simulations that for a given value of m, the dependence of B on V_g and z_0 is relatively weak (as indicated by the length of the corresponding range lines for each of the considered m values). The simulated Bowen ratio drops in the summer case from about $B \cong 14$ for $m \cong 0.01$ (very dry soil) to about $B = 0.2$ for $m = 1$ (saturated soil). The value of the Bowen ratio for $m = 1$ is in agreement with commonly observed values (e.g. Hillel, 1982). In the winter case the corresponding B values are ~ 30 and 0.3, respectively. The lower surface temperatures in the winter day as compared to the summer day resulted in, as anticipated, higher Bowen ratio values. Interestingly, the relation between m and B for the presented case is linear on a log-log scale and can be approximated as $B = 0.2m^{-0.923}$ for the summer day and as $B = 0.32\,m^{-0.954}$ for the winter day. Note that, rather than using two different power laws, Fig. 8 can be fit with $B \propto m^{-0.94}$ or better $(B-0.06) \propto m^{-1}$. For the analytical evaluations presented in section 3.3.2 one can use Equation (13) and Fig. 8 in order to translate selected F values into m values.

Finally, it is worth noting that when the soil is nearly saturated, the reduction in the daytime surface evaporation rate is generally minor during a typical period of about 2 days. Following this period, generally the reduction in the daily evaporation is noticeable (e.g. Brutsaert, 1982) which leads to a daily reduction of surface soil moisture availability by some Δm. Within the general context of the presented simulations, one can consider the daily drying effect in the second period by averaging the features obtained in the range m to $m-\Delta m$.

4.2. *Evaluation of* H_s/R_s

Like the Bowen ratio, the variation of H_s/R_s as dependent on surface wetness is considerable. H_s is a quantity that directly affects parameters important to dispersion, i.e. L, h and w^*. To the first order $L \propto H_s^{-1}$; $h \propto H_s^{1/2}$ (see Equation 10) and closely $w^* \propto (H_s h)^{1/3} \propto H_s^{1/2}$. Because of a lack of measurements needed for evaluations of H_s, the H_s value is commonly assumed to be a fraction of the readily available values of R_s (i.e. $H_s/R_s = \xi$ where ξ is a given constant). Evaluation of B as suggested in the previous subsection, and availability of R_s enables an evaluation of

ξ as suggested in the following analysis, based on the specific cases involved with the present study.

Equation (15) can be closely approximated by:

$$\beta_0 = \beta_{d_0}(1 - 0.39F), \tag{16}$$

where β_{d_0} is the 'dry' value of β_0 (i.e. $B \to \infty$). Comparing the suggested values of B with the R_{s_0} values used in the computations (see section 3.3.2), we find $\beta_{d_0}/R_{s_0} \cong 0.42$ in the summer case and ~ 0.48 in the winter case. Therefore, given other, greater uncertainties $\beta_{d_0}/R_{s_0} \cong 0.45$ is a reasonable approximation. With this, Equations (1a) and (11) imply that:

$$H_s/R_s = (1-F)\left(1 - \frac{\beta_0}{R_{s_0}}\right) \tag{17}$$

or, using Equations (13) and (16)

$$H_s/R_s = B(0.73 + 0.55B)/(1+B)^2 \cong B/(1.34 + 1.81B) \tag{18}$$

According to Equation (18) for extremely dry surfaces (i.e. $B \to \infty$), $H_s/R_s \cong 0.55$; while for saturated soil surfaces (with $B \cong 0.2$), $H_s/R_s \cong 0.12$.

4.3. *Vegetated surfaces*

Although the current study focused on the situation of bare soil surface conditions, it is worth commenting on the possible impact of a grass surface on the dispersion related features presented previously. Wilted grass (over dry soil) can be considered to be within the low range of m in the evaluations presented in the previous sections. When the grass transpires at its maximum rate (as is the common situation when the soil wetness is sufficient), the observed transpiration rates are quite similar to the evaporation rates observed over saturated soils (e.g. Jensen, 1973), and grossly the evaluations presented previously for $m = 1$ are applicable. According to Monteith (1976), the Bowen ratios observed over various canopies are typically in the range ~ 0.0–2.0 which corresponds based on Fig. 8 to $m \cong 1$–0.1.

4.4. *Advection*

Assuming a wet area is adjacent to a dry area, the advection of relatively warm air towards the wet area causes an increased thermal stabilization of the lower atmosphere and consequently to an additional suppression of the turbulence. When the wet surface is extensive (i.e. a large fetch distance) as assumed in the present study, the horizontal extent and the depth of this thermal stabilization are likely to be pronounced as can be implied, for example, from studies by Slade (1968) and Mahrer and Segal (1979). When the wet surface is of small horizontal extent (i.e. a short fetch distance) as is the case of patches of irrigated areas within a dryland, the thermal stabilization is typically limited to a few meters above the ground (e.g. Motha *et al.*, 1979).

5. CONCLUSIONS

The impact of wet surfaces on selected dispersion characteristics was studied in situations involved with extensive homogeneous areas with a uniform surface wetness. Illustrative situations typical to midlatitude summer and winter days were considered. The simulation results suggest that an extreme variation in surface moisture availability over an extensive area, may result in a change of one Pasquill stability class around noon. However, early in the morning and late in the afternoon the modification can be more substantial. A similar general conclusion was obtained when the ratio w^*/U was considered as an index for dispersion in the ABL. The impact of a change in the depth of the ABL, from very dry to an extremely wet surface, was indicated to be a factor of ~ 1.5–2. Thus, it is suggested, for example, that surface concentrations from a plume trapped within the ABL, or due to surface emissions, may be increased by a factor of 1.5–2 due to such surface moisture variations. On the other hand, the reduction in the ABL depth due to surface moistening may result in the penetration of such a plume to above the ABL capping inversion, thereby reducing significantly the surface concentrations. The last situation is most likely to occur in the morning hours, or in synoptic conditions in which the ABL is suppressed by a synoptic subsidence to the typical effective height of tall stacks.

Acknowledgements—The study was supported by EPRI under contract # RP-1630-53 and by NSF grant # ATM-8616662. Computations were carried out by the NCAR CRAY computer (NCAR is sponsored by the NSF). Constructive criticism by anonymous reviewers contributed to this paper. Section 4.2 was adopted from one of the reviewer's comment notes. We would also like to thank B. Critchfield for typing the manuscript.

REFERENCES

Atwater M. A. and Brown P. S. (1974) Numerical calculation of the latitudinal variation of solar radiation for an atmosphere of varying opacity. *J. appl. Met.* **13**, 289–297.

Briggs G. A. (1988) Surface inhomogeneity effects on convective diffusion. *Boundary-Layer Met.* **45**, 117–135.

Brutsaert W. H. (1982) Vertical flux of moisture and heat at a bare soil surface. In *Land Surface Processes in Atmospheric Circulation Models* (edited by P. S. Eagleson), pp. 115–168. Cambridge University Press, Cambridge.

Businger J. A., Wyngaard J. C., Izumi Y. and Bradley E. F. (1971) Flux-profile relationship in the atmospheric surface layer. *J. atmos. Sci.* **28**, 181–189.

Carlson T. N. and Boland F. E. (1978) Analysis of urban–rural canopy using a surface heat flux/temperature model. *J. appl. Met.* **17**, 998–1013.

De Vries D. A. (1963) Thermal properties of soils. In *Physics of Plant Environment* (edited by W. R. van Wijk), pp. 210–235. John Wiley, New York.

Golder D. (1972) Relations among stability parameters in the surface layer. *Boundary Layer Met.* **3**, 54–58.

Hillel D. (1982) *Introduction to Soil Physics.* Academic Press, New York.

Idso S. B., Jackson, R. D., Reginto R. J., Kimball F. S. and

Nakayama F. (1975) The dependence of bare soil albedo on soil water content. *J. appl. Met.* **14,** 109–113.

Jensen M. E. (1973) *Consumptive Use of Water and Irrigation Water Requirements.* American Society of Civil Engineers, New York.

Mahrer Y. and Pielke R. A. (1977) A numerical study of the airflow over irregular terrain. *Beit. Phys. Atmos.* **50,** 98–113.

Mahrer Y. and Segal M. (1979) Simulation of advective Sharav conditions over Israel. *Isra. J. Earth Sci.* **28,** 103–106.

McCumber M. C. and Pielke R. A. (1981) Simulation of the effect of surface fluxes of heat and moisture in mesoscale numerical models. *J. geophys. Res.* **86,** 9929–9938.

McNider R. T. and Pielke R. A. (1981) Diurnal boundary layer development over sloping terrain. *J. atmos. Sci.* **28,** 2198–2212.

Monteith J. L. (ed.) (1976) *Vegetation and the Atmosphere,* Vol. 2. Academic Press, New York.

Motha R. P., Verma S. B. and Rosenberg N. J. (1979) Turbulence under conditions of sensible heat advection. *J. appl. Met.* **18,** 467–473.

Myrup L. O. and Ranzieri A. J. (1976) A consistent scheme for estimating diffusivities to be used in air quality models. State of California, Dept, of Transportation, Office of Transportation Laboratory.

Nappo C. J. (1975) Parameterization of surface moisture and evaporation rate in planetary boundary layer model. *J. appl. Met.* **14,** 289–296.

O'Brien J. J. (1970) A note on the vertical structure of the eddy exchange coefficient in the planetary boundary layer. *J. atmos. Sci.* **27,** 1213–1215.

Ookouchi Y., Segal M., Mahrer Y. and Pielke R. A. (1987) On the effect of soil wetness on thermal stress. *Int. J. Biomet.* **31,** 45–55.

Pan H. L. and Mahrt L. (1987) Interaction between soil hydrology and boundary layer development. *Boundary-Layer Met.* **38,** 185–202.

Philip J. R. (1987) A physical bound on the Bowen ratio. *J. clim. appl. Met.* **26,** 1043–1045.

Pielke R. A. and Mahrer Y. (1978) Verification analysis of the University of Virginia three dimensional mesoscale prediction over south Florida for July 1, 1973. *Mon. Wea. Rev.* **106,** 1568–1589.

Sasamori T. (1972) A linear harmonic analysis of atmospheric motion with radiative dissipation. *J. met. Soc. Japan* **50,** 505–518.

Segal M. and Mahrer Y. (1979) Heat load conditions in Israel—a numerical mesoscale model study. *Int. J. Biomet.* **23,** 279–284.

Segal M. and Pielke R. A. (1981) Numerical model simulation of biometeorological heat load condition—summer day case study for the Chesapeake Bay area. *J. appl. Met.* **20,** 735–749.

Slade D. H. (1968) Atmospheric dispersion over Chesapeake Bay. *Mon. Wea. Rev.* **90,** 217–224.

Stull R. B. (1988) *An Introduction to Boundary Layer Meteorology.* Kluwer Academic Publishers, Dordrecht.

Tennekes H. (1973) A model for the dynamics of inversion above a convective boundary layer. *J. atmos. Sci.* **30,** 558–567.

Turner D. B. (1964) A diffusion stability model for an urban area. *J. appl. Met.* **3,** 83–91.

Weil J. C. and Brower R. P. (1984) An updated Gaussian plume model for tall stacks. *J. Air Pollut. Control Ass.* **34,** 818–827.

Zhang D. L. and Anthes R. A. (1982) A high resolution model of the planetary boundary layer—sensitivity tests and comparisons with SESAME-79 data. *J. appl. Met.* **21,** 1594–1609.